Potential Measurement with the 6-MeV Heavy Ion Beam Probe of LHD

Akihiro SHIMIZU, Takeshi IDO, Masaki NISHIURA, Shigetoshi NAKAMURA[1)], Harushisa NAKANO, Shinsuke OHSHIMA[2)], Akimitsu NISHIZAWA, Masayuki YOKOYAMA, Yasuo YOSHIMURA, Shin KUBO, Takashi SHIMOZUMA, Hiroe IGAMI, Hiromi TAKAHASHI, Naoki TAMURA, Ichihiro YAMADA, Takashi MINAMI, Kazumichi NARIHARA, Tsuyoshi AKIYAMA, Tokihiko TOKUZAWA, Kenji TANAKA, Kazuo KAWAHATA, Kazuo TOI, Mitsutaka ISOBE, Fumitake WATANABE, Kunihiro OGAWA[1)], Kenichi NAGAOKA, Katsunori IKEDA, Masaki OSAKABE, Katsuyoshi TSUMORI, Yasuhiko TAKEIRI, Osamu KANEKO, Shinji KATO, Mitsuhiro YOKOTA, Yasuji HAMADA and LHD Group

National Institute for Fusion Science, 322-6 Oroshi-cho, Toki, Gifu 509-5292, Japan
[1)]*Department of Energy Science and Engineering, Nagoya University, Nagoya 464-8603, Japan*
[2)]*Institute of Laser Engineering, Osaka University, 2-6 Yamadaoka, Suita, Osaka 565-0871, Japan*

(Received 3 February 2009 / Accepted 9 September 2009)

The potential in the plasma core of the Large Helical Device (LHD) was measured with the 6 MeV Heavy Ion Beam Probe (HIBP). The radial profile of the potential in the region where the normalized minor radius, ρ, is less than 0.5 was measured and the electric field obtained from the fitting function of the experimental data was compared with that calculated from neoclassical ambipolarity. The experimental results coincide well with the theoretical calculations. Negative pulses were observed in the potential signal in the inward shifted magnetic configuration. The time constants of these pulses were less than the energy confinement time. Potential fluctuations of the coherent modes were also observed, and one of their frequencies coincided with the geodesic acoustic mode (GAM). In this report, the present status of potential measurements with the HIBP system in LHD is described.

Keywords: Large Helical Device, heavy ion beam probe, potential, tandem accelerator, tandem analyzer

DOI: 10.1585/pfr.5.S1015

1. Introduction

In toroidal magnetized plasmas, a radial electric field is very important to improve performance, as observed in tokamak H-mode transitions [1–3]. In experiments on helical devices, internal transport barriers (ITB) have been observed [4–6]. Recent theoretical studies show that a transport barrier is created by a poloidal shear flow, because the shear flow can reduce anomalous transport by suppressing turbulence in the plasma [7]. The poloidal flow is related to the radial electric field through $\boldsymbol{E}\times\boldsymbol{B}$ drift, therefore, the poloidal shear flow can be estimated from the structure of the radial electric field. In helical devices, the radial electric field is dominated by the non-ambipolar flux in neoclassical context, so it is also important to study the effect of neoclassical theory on the radial electric field experimentally. In order to study the physics in an experimental device in detail, we need to measure the structure of the radial electric field with good accuracy and spatial/temporal resolution.

The Heavy Ion Beam Probe (HIBP) [8] is a very useful tool for studying the physics related to radial electric fields, because it can directly measure the plasma potential inside a high temperature toroidal plasma with good spatial/temporal resolution, without disturbing the plasma. In order to measure the radial structure of a potential and its fluctuation in the Large Helical Device (LHD), the 6-MeV Heavy Ion Beam Probe was installed and has been developed [9, 10]. Details of the system are shown in the references, so only a brief explanation will be given in section 2. Recently the amplifier of the beam detector was enhanced and the temporal resolution was improved up to 500 kHz (compared to ∼20 kHz for the previous amplifier).

In this report, the present status of the HIBP in LHD is described and recent results obtained using the system are presented. To date, the system has been operated at an acceleration energy of 6 MeV, however the resolution of potential measurements was not good because the acceleration voltage was not stable above ∼1.3 MV (corresponding to 2.6 MeV). Therefore, most of the data shown here were obtained for an acceleration voltage less than 1.3 MV.

2. HIBP System in LHD

Figure 1 shows a schematic view of the HIBP sys-

author's e-mail: akihiro@nifs.ac.jp

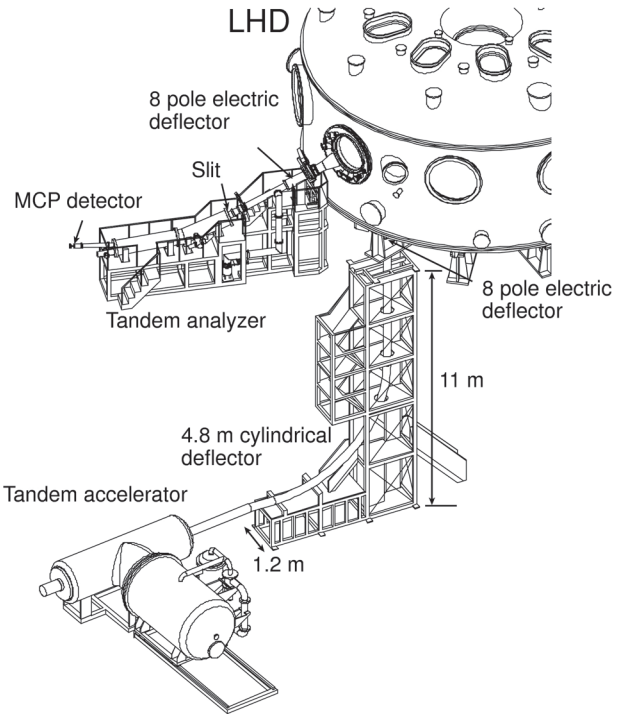

Fig. 1 Schematic view of HIBP system in LHD. The negative ion source is omitted in this figure.

tem in LHD. The toroidal magnetic field strength of LHD is 3 T and the typical major/minor radius is 3.6 m / 0.6 m. An acceleration energy of 6 MeV is required to inject a Au^+ probing beam into the center of a plasma. To reduce the required voltage by half, a tandem accelerator is used in our system. Negative ions, Au^-, are produced in the target sputter ion source [11], and are extracted and pre-accelerated up to 50 keV. Then, the beam is injected into the tandem accelerator and accelerated to 3 MeV. In the gas cell located at the center of the tandem accelerator, the Au^- ions are stripped of two electrons and changed to positive ions, Au^+. These ions are re-accelerated to 6 MeV. This beam is then guided to the plasma through several components: a charge separator, a 4.8-m cylindrical deflector, a 7.8-degree deflector, and other components. The orbit of the probing beam has a three-dimensional structure in the plasma. The injection and ejection angles of the probing beam are controlled by two eight-pole electric deflectors (sweepers) at the injection and ejection ports. By controlling these angles, the observation point is changed. The injected Au^+ are stripped of an electron by collision with the plasma and gain potential energy at this ionization point. We call the Au^+ beam the primary beam and the produced Au^{2+} beam the secondary beam. By measuring the difference in energy between the primary and secondary beams, the plasma potential at the ionization point can be measured.

The ionization point lies within a sample volume. The positions of the sample volumes are arranged three-dimensionally in the plasma, because that the beam orbit has three-dimensional geometry. The projection of the sample volume positions on a vertically elongated cross section is shown in Fig. 2 for a toroidal magnetic field strength of 1.5 T, major radius of the magnetic axis of 3.75 m, and acceleration energy of 1.376 MeV. The size of a sample volume (spatial resolution) is about a few cm (~2.5 cm) [12]. Our HIBP system can measure the potential within the normalized minor radius from 0 to 0.5.

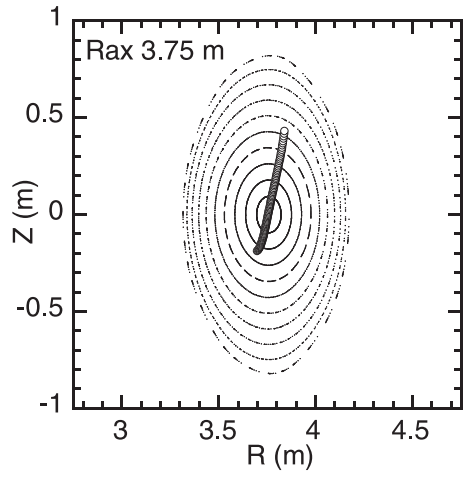

Fig. 2 Projection of sample volume positions on a vertically elongated cross section and magnetic surfaces for the configuration R_{ax} 3.75 m.

For a traditional Proca-Green type energy analyzer [13], the required voltage is 500 kV to 1 MV for a beam energy of 6 MeV. The electric power supply for this voltage is unreasonably costly. Therefore, a tandem type energy analyzer [14] is used in our system. With this analyzer, the required voltage is reduced to 120 kV, keeping the second order focusing property of the beam injection angle. The entrance of the analyzer has three slits, so the potential of three neighboring sample volumes can be measured. To detect the secondary beam current, a high gain detector with micro channel plates (MCPs) is used, which can detect a very small secondary beam current. The detected current is converted to an electric voltage signal through an electric amplifier with a temporal resolution of 500 kHz. The time resolution of our system is mainly determined by this amplifier. In LHD, the order of the detected current is about a few tens of pA or nA. The ratio of the detected secondary beam current to the injected primary beam current is 10^{-5}-10^{-4} in the density range 0.5-1.0 $\times$ 10^{19} m^{-3}. In order to measure the fluctuation, a large signal to noise (S/N) ratio is required. Therefore it is possible only in the low density case, when the line averaged electron density is less than 0.5×10^{19} m^{-3}, because the attenuation of the beam current is small. The equilibrium value of the potential and the radial profile can be measured for higher densities, though less than 1.5×10^{19} m^{-3}. For densities higher than this value, the attenuation of the probing beam current becomes strong and potential measurements are difficult with our present system.

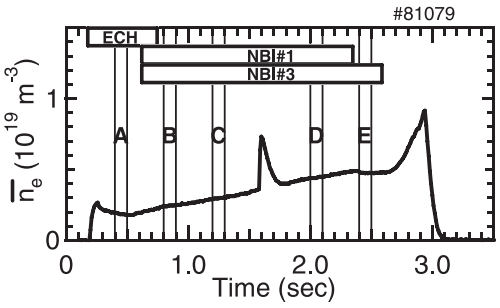

Fig. 3 Temporal evolution of the line averaged electron density, with the heating methods indicated. The potential was measured in the periods A to E.

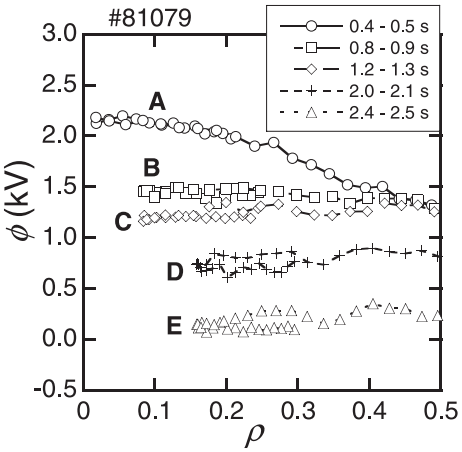

Fig. 4 Radial profiles of potential measured with HIBP. A to E correspond to the periods in Fig. 3.

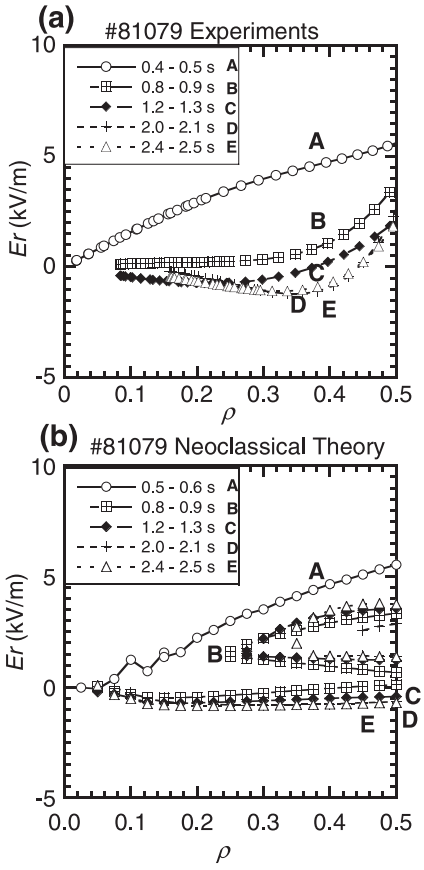

Fig. 5 (a) Radial profiles of the radial electric field obtained from the derivatives of the fitting functions of the experimental data. (b) Radial profiles of the radial electric field calculated from neoclassical theory.

3. Radial Profile of Potential

Using our HIBP system, we measured the radial profile of the potential. The magnetic configuration of LHD can be characterized by the major radius of the axis R_{ax}, the toroidal magnetic field strength B_t, the pitch parameter γ, and the quadrupole component of the magnetic field B_q. The radial potential profile was measured in a standard magnetic field configuration, $R_{ax} = 3.75$ m, $B_t = 1.5$ T, $\gamma = 1.254$, $B_q = 100\,\%$. The energy of the probing beam was 1.376 MeV. The plasma was produced by electron cyclotron heating (ECH) and sustained by neutral beam injection heating (NBI). The line averaged density was about 0.2×10^{19} m^{-3} at the ECH phase, and it gradually increased. Figure 3 shows the temporal evolution of the line averaged density, with the heating methods indicated. The central temperature was about 2.5 keV in the ECH phase and 1.0 keV in the NBI phase. The position of the sample volume was changed by changing the injection angle of the probing beam at 10 Hz. The radial profiles of the potential obtained from HIBP in the periods A to E are shown in Fig. 4. In the ECH phase, the potential was positive at the center. In the NBI phase, the potential at the central region was positive, and it decreased as the density increased.

By fitting these experimental data with polynomial functions and differentiating, the profiles of the electric field were obtained. They are compared with neoclassical theory in Fig. 5. Figure 5 (a) shows the radial profile of the electric field obtained from the fitting function of the experimental results and Fig. 5 (b) shows the calculation results estimated by using the GSRAKE code [15], which calculates the radial electric field based on neoclassical theory. In Fig. 5 (b), in the region where $\rho > 0.25$ in B to E, multiple roots exist. In this region, the largest positive root corresponds to the electron root, and the smallest negative or almost zero root corresponds to the ion root. The root between these is the unstable root. The experimental results are largely consistent with the neoclassical calculation results. In the ECH phase (case A), a positive electric field was observed, which corresponds to the electron root in the theory. In the NBI phase (cases B-E), a small negative electric field was observed in the core region, which corresponds to the ion root in the theory. Hence we can conclude that the electric field in the core region of this experiment can be almost determined by neoclassical theory.

4. Negative Pulses Observed in Potential Signal

For the inward shifted configuration, negative pulses

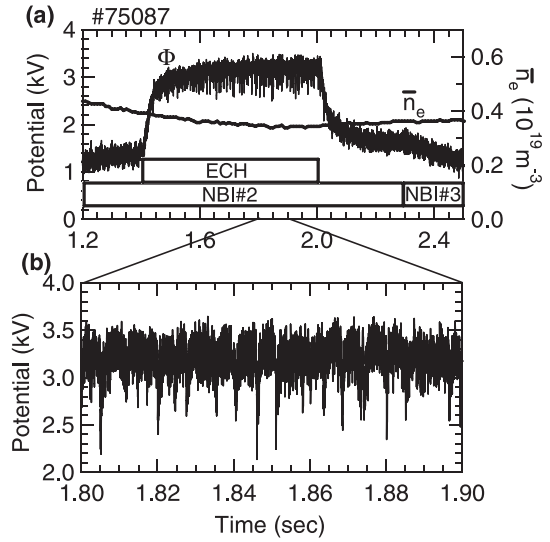

Fig. 6 (a) Temporal evolutions of the potential Φ and line averaged density $\bar{n}_e$ based on the heating method. (b) Magnification of potential signal from 1.8 to 1.9 sec.

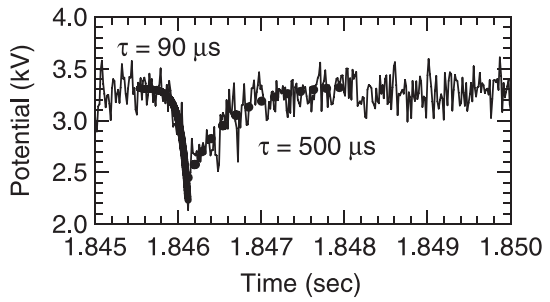

Fig. 7 Time constants τ of negative pulses. These are faster than the energy confinement time.

were observed in the potential signal. The parameters for this magnetic configuration were as follows: $R_{ax} = 3.6$ m, $B_t = 1.5$ T, $\gamma = 1.254$, $B_q = 100\,\%$. In this case, the probing beam energy of HIBP was 1.562 MeV. Plasma was produced and sustained by co-injection NBI heating. The temporal evolutions of the line averaged density and potential are shown in Fig. 6 (a), with the heating methods indicated. The line averaged density is about 0.4×10^{19} m^{-3}. At 1.4 sec, ECH was additionally applied. In the ECH phase, negative pulses were observed, as shown in Fig. 6 (b). The normalized minor radius of the sample volume position was fixed at ~0.4. Negative pulses can be seen in the temporal evolution of the potential signal. Typical time constants are 90 μs in the drop phase and 500 μs in the recovering phase, as shown in Fig. 7. The energy confinement time is ~100 ms in LHD. The time constants of the negative pulses were much faster than the energy confinement time, so these negative pulses are considered to be due to bifurcation of the electric field. They were observed only in the inward shift case, $R_{ax} = 3.6$ m, and at low density ($n_e < 0.5 \times 10^{19}$ m^{-3}). They were not observed in other configurations ($R_{ax} > 3.75$ m) or at high density. The reason for this may be the difference in the configuration properties in the context of neoclassical theory.

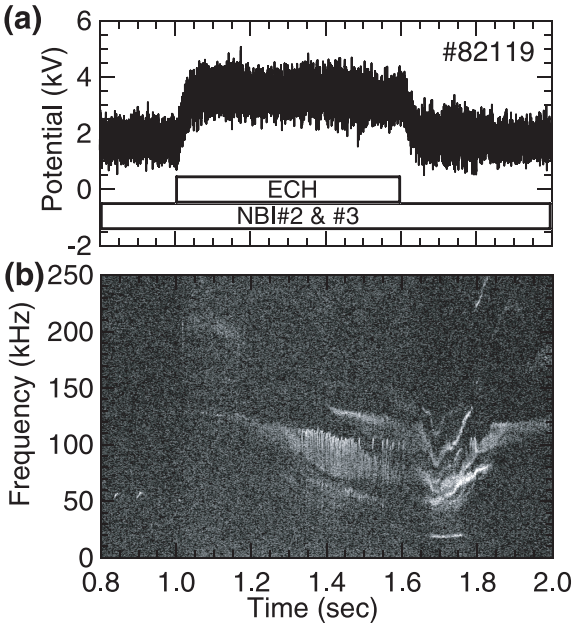

Fig. 8 (a) Temporal evolution of the potential, with the heating methods indicated. (b) Spectrogram of potential fluctuation.

In compact helical system (CHS), such bifurcation phenomena has been observed [16, 17] and are referred to as "pulsation", various types of which have been observed. At low density, a large drop in potential is observed. The potential at the center in the additional ECH phase is ~1 kV in the electron root, dropping to a few hundred V in the ion root. The change of potential is ~1 kV. However, at high density in CHS, the drop in potential is small, about 100-200 V. The result for LHD is similar to the high density case for CHS. The time constant of the negative pulses in LHD is of the same order as the pulsation in CHS.

5. Observation of Coherent Modes

We have improved the amplifier of the detector, increasing the S/N ratio of the fluctuation measurements. In the potential signal, fluctuation caused by the coherent modes was observed. In Fig. 8 (a), the temporal evolution of the potential is shown, when the fluctuation caused by the coherent modes was measured, with the heating methods indicated. In this case, the plasma was produced and sustained by NB heating. The line averaged density was about 0.1×10^{19} m^{-3}, which is relatively low. ECH was applied from 1.0 to 1.6 sec, injected for the co-directed current drive.

In Fig. 8 (b), a spectrogram of the potential signal is shown. The position of the sample volume was $\rho \sim 0.3$. The signals had coherence with the signals of the magnetic probes and are therefore considered to be coherent modes caused by MHD instabilities. In this case, the rotational transform at the central region was increased by the

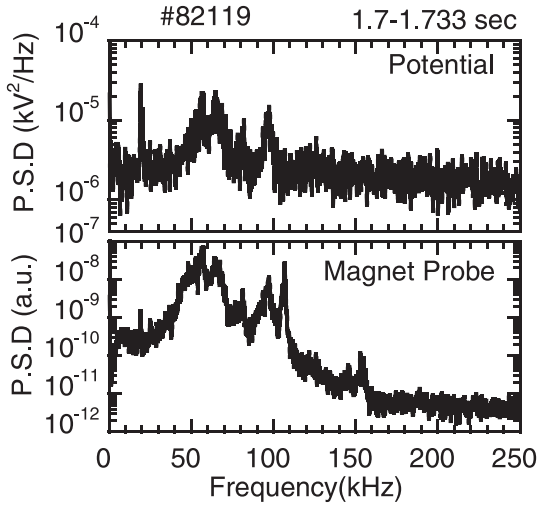

Fig. 9 Upper: Power spectrum density of potential signal in the time period 1.7-1.733 sec. Lower: Power spectrum density of the magnetic probe signal, $\dot{B}$, in the same period.

ECH current drive and the shear in the rotational transform profile in the central regime became small. It is considered that some sort of Alfven Eigen modes were excited in this case. The power spectrum densities of the potential and magnetic probe signals in the period from 1.7 to 1.733 sec are shown in Fig. 9. The peak around the frequency of 60 kHz in both signals is considered to be due to Alfven Eigen modes. Around a frequency of 20 kHz, a fluctuation having a constant frequency is seen, which coincides with the frequency of the geodesic acoustic mode (GAM) [18, 19]. This peak can be seen more clearly in the potential signal than in the magnetic probe. This mode is localized in the central region of the plasma [20]. The fluctuation amplitude was several hundreds volts.

To date, fluctuation caused by turbulence has not been measured clearly in the potential signal, because the S/N ratio of our system is not sufficient. A further improvement in the S/N ratio is therefore needed in the future.

6. Summary

A 6-MeV Heavy Ion Beam Probe has been developed for LHD. For acceleration energies of less than 2.6 MeV, the acceleration energy is stable, so the potential in the plasma can be measured with a good S/N ratio. The radial potential profile was measured in the magnetic field configuration R_{ax} = 3.75 m of LHD. The experimental results were compared with neoclassical theory. The radial profile of the electric field obtained from the experiment coincides well with the theoretical calculation. In the inward shifted configuration (R_{ax} = 3.6 m), negative pulses were observed in the potential signal. The fluctuations of the coherent modes were measured with the HIBP. The frequency of one of them coincided with the GAM. Its amplitude was about several hundred volts.

Acknowledgments

This work was supported by the NIFS budget under contract no. ULBB 505, 514, 515, and was supported in part by MEXT Japan under Grants-in-Aid for Young Scientists (Nos. 16760674, 18760640) and NIFS/NINS under the Project of Formation of International Network for Scientific Collaborations. The authors wish to thank the scientific and technical staff of LHD for their continual support.

[1] R.J. Groebner, K.H. Burrell, R.P. Seraydarian *et al.*, Phys. Rev. Lett. **64**, 3015 (1990).
[2] K. Ida, S. Hidekuma, Y. Miura, T. Fujita, M. Mori, K. Hoshino, N. Suzuki, T. Yamauchi *et al.*, Phys. Rev. Lett. **65**, 1364 (1990).
[3] T. Ido, K. Kamiya, Y. Miura, Y. Hamada, A. Nishizawa and Y. Kawasumi, Phys. Rev. Lett. **88**, 055006 (2002).
[4] A. Fujisawa, H. Iguchi, T. Minami, Y. Yoshimura, H. Sanuki, K. Itoh, S. Lee, K. Tanaka *et al.*, Phys. Rev. Lett. **82**, 2669 (1999).
[5] A. Fujisawa, H. Iguchi, T. Minami, Y. Yoshimura, K. tanaka, K. Itoh, H. Sanuki, S. Lee, M. Kojima, S.-I. Itoh, M. Yokoyama, S. Kado, S. Okamura, R. Akiyama, K. Ida *et al.*, Phys. Plasmas **7**, 4152 (2000).
[6] T. Estrada, A. Alonso, A.A. Chmyga, N. Dreval, L. Eliseev, C. Hidalgo, A.D. Komarov, A.S. Kozachok *et al.*, Plasma Phys. Control. Fusion **47**, L57 (2005).
[7] K.H. Burrell, Phys. Plasmas **4**, 1499 (1997).
[8] T.P. Crowley *et al.*, IEEE Trans. Plasma Sci. **22**, 291 (1994).
[9] T. Ido, A. Shimizu, M. Nishiura, A. Nishizawa, S. Katoh, K. Tsukada, M. Yokota, H. Ogawa, T. Inoue, Y. Hamada *et al.*, Rev. Sci. Instrum. **77**, 10F523 (2006).
[10] A. Shimizu, T. Ido, M. Nishiura, H. Nakano, I. Yamada, K. Narihara, T, Akiyama, T. Tokuzawa, K. Tanaka *et al.*, J. Plasma Fusion Res. **2**, S1098 (2007).
[11] M. Nishiura, T. Ido, A. Shimizu, S. Kato, K. Tsukada, A. Nishizawa, Y. Hamada, Y. Matsumoto *et al.*, Rev. Sci. Instrum. **77**, 03A537 (2006).
[12] T. Ido, A. Shimizu, M. Nishiura, Y. Hamada, S. Kato, A. Nishizawa and H. Nakano, J. Plasma Fusion Res. **2**, S1100 (2007).
[13] G.A. Proca and T.S. Green, Rev. Sci. Instrum. **41**, 1778 (1970).
[14] Y. Hamada, A. Fujisawa, H. Iguchi, A. Nishizawa and Y. Kawasumi, Rev. Sci. Instrum. **68**, 2020 (1997).
[15] C.D. Beidler, W.D. D'haeseleer, Plasma Phys. Control. Fusion **37**, 463 (1995).
[16] A. Fujisawa, H. Iguchi, H. Idei, S. Kubo, K. Matsuoka, S. Okamura, K. Tanaka, T. Minami, S. Ohdachi, S. Morita, H. Zushi *et al.*, Phys. Rev. Lett. **81**, 2256 (1998).
[17] A. Fujisawa, H. Iguchi, T. Minami, Y. Yoshimura, K. Tanaka, K. Itoh, H. Sanuki, S. Lee, M. Kojima, S.-I. Itoh *et al.*, Phys. Plasmas **7**, 4152 (2000).
[18] N. Winsor, J.L. Johnson and J.M. Dowson, Phys. Fluids **11**, 2448 (1968).
[19] P.H. Diamond, S.-I. Itoh, K. Itoh and T.S. Hahm, Plasma Phys. Control. Fusion **47**, R35 (2005).
[20] T. Ido, A. Shimizu, M. Nishiura, H. Nakano, S. Ohshima, S. Kato, Y. Hamada, Y. Yoshimura, S. Kubo, T. Shimozuma, H. Igami, H. Takahashi, K. Toi *et al.*, Rev. Sci. Instrum. **79**, 10F318 (2008).